Original Article

Lanatoside C induces ferroptosis in non-small cell lung cancer *in vivo* and *in vitro* by regulating SLC7A11/GPX4 signaling pathway

Yaozong Xia[1#], Teng Liu[1,2#], Shihua Deng[2], Li Li[1], Jin Li[1], Feng Zhang[1], Shuang He[1], Wei Yuan[1], Dongming Wu[1,2], Ying Xu[1,2]

[1]School of Clinical Medicine, Chengdu Medical College, Chengdu, China; [2]Department of Laboratory Medicine, the First Affiliated Hospital of Chengdu Medical College, Chengdu, China

Contributions: (I) Conception and design: Y Xu, D Wu; (II) Administrative support: T Liu, J Li; (III) Provision of study materials or patients: Y Xia, S Deng; (IV) Collection and assembly of data: L Li, F Zhang; (V) Data analysis and interpretation: S He, W Yuan; (VI) Manuscript writing: All authors; (VII) Final approval of manuscript: All authors.

[#]These authors contributed equally to this work.

Correspondence to: Ying Xu, MD; Dongming Wu, MD. School of Clinical Medicine, Chengdu Medical College, Chengdu, China; Department of Laboratory Medicine, the First Affiliated Hospital of Chengdu Medical College, 278 Baoguang Avenue, Xindu District, Chengdu 610500, China. Email: yingxu882255@sina.com; harvey1989@126.com.

Background: Non-small cell lung cancer (NSCLC) is a common malignant tumor worldwide, remaining resistant to chemotherapy drugs. Lanatoside C can inhibit the growth of cancer cell lines. In this study we aimed to investigate the relationship between lanatoside C and ferroptosis, exploring the possible mechanism in NSCLC.

Methods: Experiments *in vitro* and *in vivo* were conducted. A549 cells were used for in vitro, including cell counting kit-8 (CCK-8) assay, lactate dehydrogenase (LDH) release, western blotting, flow cytometry, transmission electron microscopy (TEM), and confocal microscopy. *In vivo*, a subcutaneous tumor model in nude mice using A549 cells was built and body size of the mice was observed. Ki67 immunohistochemistry, hematoxylin-eosin (HE) staining, and western blotting were conducted respectively.

Results: The results showed that lanatoside C had an inhibitory effect on the growth of A549 cells, and the dose of lanatoside C used in this experiment was set at 0.4 μM for 24 hours. When A549 cells were treated with lanatoside C, the cell viability was decreased observably ($P<0.001$) and LDH release was significantly enhanced ($P<0.01$) compared with the control group. However, when A549 cells were treated together with lanatoside C and five different inhibitors, containing ferroptosis inhibitors, necroptosis inhibitors, apoptosis inhibitors, pyroptosis inhibitors, and autophagy inhibitors, the results showed that the viability of A549 cells with lanatoside C and ferrostatin-1 (Fer-1) was reduced ($P>0.05$) and the LDH release was significantly enhanced ($P<0.05$). Besides, TEM and confocal microscopy showed that the mitochondria of A549 cells in the lanatoside C group disappeared and the mitochondrial membrane potential decreased. *In vivo*, lanatoside C efficiently enhanced the sensitivity of the xenograft tumors, as well as reducing the size and weight of the tumor. Moreover, immunohistochemical staining analysis revealed that the SLC7A11 and GPX4 levels significantly decreased in the lanatoside C group. In addition, the expression of GPX4 and SLC7A11 by western blotting was decreased in lanatoside C group.

Conclusions: Collectively, lanatoside C could inhibit the proliferation and induce ferroptosis, and have a biological effect on inducing ferroptosis in NSCLC.

Keywords: Lanatoside C; ferroptosis; non-small cell lung cancer (NSCLC); SLC7A11; GPX4

Submitted Dec 13, 2023. Accepted for publication Apr 11, 2024. Published online May 28, 2024.
doi: 10.21037/tcr-23-2285
View this article at: https://dx.doi.org/10.21037/tcr-23-2285

Introduction

Lung cancer is one of the most common malignant tumors in China, among which non-small cell lung cancer (NSCLC) accounts for about 85% (1), and more than 70% of NSCLC patients are already in advanced stage at initial diagnosis and cannot be treated surgically (2). As one of the common treatments, chemotherapy is useful for NSCLC patients with advanced age or poor clinical performance. However, a great challenge to the efficacy of chemotherapy comes out due to treatment resistance (3). Therefore, it is important to explore therapeutic drugs for NSCLC to improve the targeted diagnosis and treatment.

It is reported that many chemotherapeutic drugs may play a part in resisting NSCLC by regulating ferroptosis (4). Ferroptosis is an iron-dependent programmed cell death mediated by massive lipid peroxidation (5,6). It is crucial for the control or the treatment or the development of various diseases such as acute lung and kidney injuries (7-9). The induction of ferroptosis can lead to a restriction of tumor cell growth and significantly improve the therapeutic outcome of tumors. Recent studies have found that ferroptosis plays a critical role in both malignant progression and treatment of NSCLC. For example, ferroptotic damage triggers inflammation-associated immunosuppression in tumor microenvironment (10); erastin, as an inducer of heterologous ferroptosis, exhibits significant tumor growth inhibition effects in lymphoma models (11); bufotalin induces ferroptosis in NSCLC cells by facilitating the ubiquitination and degradation of GPX4 (12); and Nrf2/heme oxygenase-1 signaling pathway and thereby inhibits NSCLC cell growth (13). These findings suggested that ferroptosis may play a key role in the development of NSCLC, and the ferroptosis regulatory proteins such as SLC7A11 and GPX4 may be important regulators in the process of the progress of malignant of NSCLC. As a result, exploring the mechanisms of ferroptosis in the process of cancer makes it significance for cancer therapy, so there is an urgent need to find new NSCLC drugs that may induce ferroptosis.

Lanatoside C is one of the cardiac glycosides (14-16), which is used in clinical practice to treat heart failure by inhibiting sodium-potassium pump. In recent years, the anti-cancer effect of lanatoside C has been gradually explored, and a previous study reported that in cancer cell lines lanatoside C could inhibit cell proliferation and induce apoptosis (17). In addition, it has been demonstrated that lanatoside C can control the development of liver cancer by accelerating apoptosis and slowing down the rate of tumor metastasis in nude mice, and tumor cells are more susceptible to cardiac glycosides than normal cells (18,19). Unfortunately, the mechanism of the inhibiting effect of lanatoside C on lung cancer has not been reported.

There is a lack of evidence that whether the inhibiting effect of lanatoside C on lung cancer is related to ferroptosis. So, in this study we aimed to investigate the relationship between the inhibiting effect of lanatoside C and ferroptosis *in vitro* and *in vivo*, and explore the possible mechanism of the action, which is beneficial to the provision of new therapeutic insights for NSCLC. A protocol was prepared before the study without registration. We present this article in accordance with the ARRIVE reporting checklist (available at https://tcr.amegroups.com/article/view/10.21037/tcr-23-2285/rc).

Highlight box

Key findings

- We investigated the relationship between the inhibiting effect of lanatoside C and ferroptosis, and explored the possible mechanism of the action, which is beneficial to the provision of new therapeutic insights for non-small cell lung cancer (NSCLC).

What is known and what is new?

- In cancer cell lines lanatoside C could inhibit cell proliferation and induce apoptosis. It can control the development of liver cancer by accelerating apoptosis and slowing down the rate of tumor metastasis in nude mice.
- In this study we aimed to investigate the relationship between lanatoside C and ferroptosis, exploring the possible mechanism in NSCLC.

What is the implication, and what should change now?

- Experiments *in vitro* and *in vivo* were conducted. A549 cells were used for *in vitro*, including cell counting kit-8 assay, lactate dehydrogenase release, western blotting, flow cytometry, transmission electron microscopy and confocal microscopy. *In vivo*, a subcutaneous tumor model in nude mice using A549 cells was built. Body size of the mice was observed, Ki67 immunohistochemistry was conducted, and hematoxylin-eosin staining was carried out.

Methods

Cell line and culture

The human NSCLC cell line A549 was purchased from the American Type Culture Collection. A549 cell line was removed from the liquid nitrogen storage tank, immediately

placed in a 37 ℃ water bath, shook for 1 min, and observed until completely melted. An appropriate amount of penicillin-streptomycin was added, and A549 cell line was incubated in 5% CO_2, 37 ℃. When the adherent cell coverage reached 70–80%, 3 mL phosphate-buffered saline (PBS) was used to rinse for three times. One mL 0.25% pancreatic enzyme was included to cover the bottom for digestion for 2 min, and the cells were maintained in RPMI-1640 medium with 10% fetal bovine serum at 37 ℃ with 5% CO_2 to terminate digestion, along with being centrifuged at 1,000 rpm at 4 ℃ for 3 min. Two mL of complete medium was added to resuspend the cells, which were transferred to a new cell culture at a ratio of 1:10, and 8 mL RPMI-1640 medium with 10% fetal bovine serum also was put into it. The cell line was incubated at 37 ℃ with 5% CO_2.

To explore the anti-proliferative effect of lanatoside C, A549 cells were divided into six groups, five of which were each given a different inhibitor into the medium during the incubation, for example, the control group (without an inhibitor), Z-VAD-FMK (an inhibitor for apoptosis) group, necrosulfonamide (an inhibitor for necrocytosis) group, VX-765 (an inhibitor for pyroptosis) group, ferrostatin-1 (Fer-1; an inhibitor for ferroptosis) group, and 3-MA (an inhibitor for autophagy) group.

Cell counting kit-8 (CCK-8) assay

Ten μL mixed cell suspension was added to a beef counting plate, and according to the counting results the 100 μL cell suspension was needed to be inoculated in each well. The 100 μL cell suspension was seeded into the 96-well plate, and then put into the conventional incubator at 37 ℃ and 5% CO_2 for 24 hours. When the cells grew completely, they were divided into nine groups: control group and lanatoside C group (0.05, 0.1, 0.2, 0.3, 0.4, 0.5, 0.6, 0.7 μM). For detection, 100 μL fresh medium containing 10 μL CCK-8 solution (Beyotime, Shanghai, China) was added to each plate and incubated for 1 hour. Absorbance at 450 nm was detected using microplate reader, which could indirectly reflect the number of living cells according to the change of absorbance.

Lactate dehydrogenase (LDH) release

Cells were inoculated in 96-well plates at the density of 1×10^4 per well and incubated overnight. After receiving the corresponding treatments, the LDH release assay was performed using the LDH Cytotoxicity Assay Kit (Beyotime) according to the manufacturer's instructions.

Western blotting

Total proteins were extracted using radioimmunoprecipitation assay buffer. Proteins were separated according to molecular weight using 8% sodium dodecyl sulfate-polyacrylamide gel electrophoresis (SDS-PAGE) and transferred onto polyvinylidene fluoride membranes. The membranes were immersed in 5% skimmed milk for 2 hours at 25 ℃ and then incubated with the primary antibodies [SLC7A11 (1:6,000), GPX4 (1:4,000), β-actin (1:5,000)] overnight at 4 ℃. After washing with tris-buffered saline tween (TBST) three times, the secondary antibody (1:8,000 dilution) was added and incubated at 25 ℃ for 2 hours. After washing with TBST three times, the expression of proteins was visualized by chemiluminescence.

Flow cytometry

Pyroptosis was measured using flow cytometry. Cells were seeded into six-well plates with indicated treatments, after which the cells were trypsinized in 0.25% trypsin, and washed thrice with PBS. Then the cells were stained with 7-AAD for 15 min, and 450 μL binding buffer was added, followed by incubation with 1 μL Annexin V-phycoerythrin (PE) at 37 ℃ in the dark for 15 min. Finally, the samples were examined with a flow cytometer (FACSCalibur, BD, Franklin Lakes, NJ, USA).

Transmission electron microscopy (TEM)

The cells were prefixed with 3% glutaraldehyde and post-fixed in 1% osmium tetroxide, dehydrated in series acetone, and then infiltrated in Epox 812 and embedded in it. The semithin sections were stained with methylene blue, and ultrathin sections were cut with diamond knife, stained with uranyl acetate and lead citrate. The sections were examined with the JEM-1400-FLASH TEM.

Confocal microscopy

The cells were inoculated in 24-cell plates to make cell climbing sheets. After adherent growth, the cells were treated with drugs for 24 hours. Then, 0.5 mL/well tetramethylrhodamine ethyl ester (TMRE) staining solution was added for 20 min, and washed with PBS thrice. Then, the atomic nucleus was dyed with 4,6-diamino-2-

phenylindole (DAPI) in the installation medium, and images were obtained using the confocal laser scanning microscope (Nikon, Tokyo, Japan).

Xenograft nude mice model

Experiments were performed under a project license (No. CMC-IACUC-2022050) granted by the Experimental Animal Ethics Committee of Chengdu Medical College, in accordance with the Chengdu Medical College's guidelines for the care and use of animals. Female nude mice (BALB/c, 5–6 weeks) were purchased from GemPhamatech Limited (Chengdu, China) and kept under controlled temperature and specific pathogen-free (SPF) conditions and the cage, bedding and drinking water were autoclaved and replaced regularly. For the xenograft tumor growth assay, each mouse was subcutaneously injected with 4×10^6 cells into the right armpit. On the 10th day after tumor inoculation, 12 mice were randomly divided into three treatment groups: control group; low-dose lanatoside C group (4 mg/kg/day, dissolved in solvent); high-dose lanatoside C group (8 mg/kg/day, dissolved in solvent) for 4 weeks. To guarantee biological duplication, the mice number of each group was four (n=4). The body weight and tumor volume were measured every 7 days. The tumor volume (mm^3) was calculated according to the following formula: volume = (length × $width^2$)/2. At the end of the study, the mice were anesthetized with 0.3% sodium pentobarbital by intraperitoneally injected at 50–60 mg/kg, and performed a cervical dislocation resulting in death. Moreover, the tissue was carefully removed for further study.

Hematoxylin-eosin (HE) staining

The tumor tissue was dehydrated and transparent, and then the tissue was immersed in melted paraffin at 65 ℃ for 4 hours to be embedded. The embedded tissue was placed on a low-temperature plate for pre-cooling and then sliced conventionally, with a thickness of 5 μm. Suitable and complete slices were selected and placed at 65 ℃ for 2 hours, therewith dewaxed immediately (xylene I 10 min, xylene II 10 min, 100% ethanol I 2 min, 100% ethanol II 2 min, 95% ethanol 2 min, 85% ethanol 2 min, respectively, 75% ethanol 2 min), placed in a shaker and rinsed with distilled water for three times (each time for 3 min). The dyeing process was followed by using hematoxylin for 4 min, then washing with running water for 10 min, eosin for 20 s, and running water for 60 s. After dyeing, the slides were left at room temperature to dry, sealed with a neutral resin, fixed, and then viewed under a microscope to take photos.

Ki67 immunohistochemical staining

The selected tissue slices were put into the sheet oven to be dewaxed for 2 hours, and immediately transferred into xylene for 10 min; Then soaking in 100%, 100%, 95%, 85%, 75% ethanol, each step was processed for 5 min; Finally, distilled water was used to wash for three times (each time for 5 min). Antigen repair was carried out in high-pressure steam for 10 min, then cooled to room temperature and washed for three times by PBS with 5 min each time. Then 3% H_2O_2 was added to block the non-specific antigen of the section tissue, and was incubated at room temperature for 10 min away from light to inhibit endogenous peroxidase interference, subsequently with PBS for washing three times, 5 min each time. Then the tissue slices were boiled in citrate buffer (pH: 6.0) for antigen retrieval and blocked with 5% goat serum at 37 ℃ for 1 hour. The tissues were then incubated with the primary antibodies at 4 ℃ overnight, and incubated with the secondary antibodies. To visualize the immunocomplexes, diaminobenzidine (DAB) was used as the chromogen.

Statistical analysis

Each experiment was performed independently at least thrice. Statistical significance was determined using an unpaired Student's *t*-test for comparisons between the two groups. Experimental results were statistically analyzed using a one-way analysis of variance or two-way analysis of variance with Tukey's multiple comparison post-hoc test. All statistical analyses were performed with the GraphPad Prism 7 software (San Diego, CA, USA) and were presented as the mean ± standard deviation (SD). Statistical significance was set at $P<0.05$.

Results

Lanatoside C suppressed the growth of lung cancer cells

The structure of lanatoside C is shown in *Figure 1A*. To explore the effect of lanatoside C on lung cancer cells, different concentrations of lanatoside C were added to A549 cells, and the results showed that lanatoside C reduced the cell viability (*Figure 1B*), increased the release of LDH (*Figure 1C*) and decreased the clone formation of A549 cells (*Figure 1D*) in a dose-dependent manner. In addition,

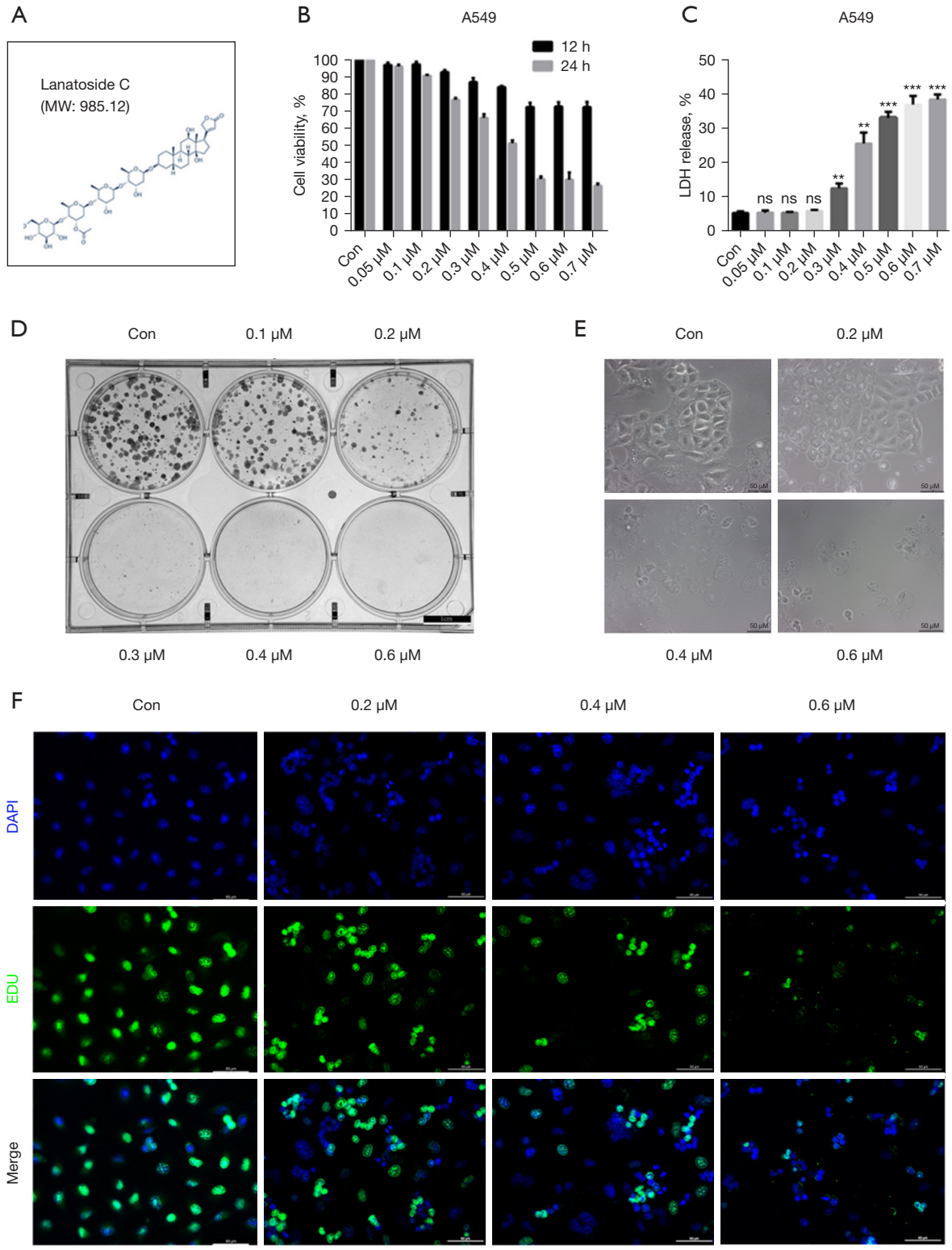

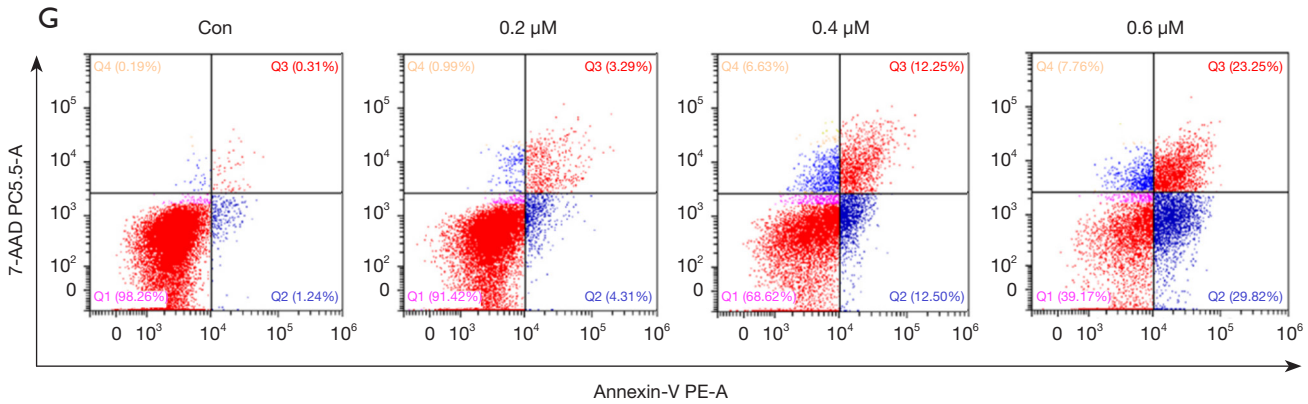

Figure 1 The effect of lanatoside C on lung cancer cells. (A) Chemical structure of lanatoside C. (B) Cell viability was assessed using CCK-8 assay at different lanatoside C concentrations. (C) The LDH release was evaluated at different lanatoside C concentrations. (D) Clone formation was observed at different lanatoside C concentrations by clone formation assay. Scale bar =1 cm. (E) The morphology of A549 cells was detected at different lanatoside C concentrations by TEM. Scale bar =50 μm. (F,G) Assessments of EDU staining by confocal microscopy (F) and flow cytometry (G) were conducted in A549 cells with lanatoside C at different concentrations. Scale bar =50 μm. Data was presented as mean ± SD, and statistical significance was calculated using one-way ANOVA with Tukey's multiple comparison test. ns, P>0.05; **, P<0.01; ***, P<0.001. MW, molecular weight; Con, control group; LDH, lactate dehydrogenase; DAPI, 4,6-diamino-2-phenylindole; EDU, 5-ethynyl-2'-deoxyuridine; PE, phycoerythrin; CCK-8, cell counting kit-8; TEM, transmission electron microscopy; SD, standard deviation; ANOVA, analysis of variance.

lanatoside C significantly changed the morphology of A549 cells (*Figure 1E*). 5-ethynyl-2'-deoxyuridine (EDU) staining and flow cytometry showed that lanatoside C significantly enhanced A549 cell death (*Figure 1F,1G*). In conclusion, lanatoside C had an inhibitory effect on the growth of A549 cells, and the dose of lanatoside C used in this experiment was set at 0.4 μM for 24 hours.

Lanatoside C induced ferroptosis of lung cancer cells

To further evaluate how lanatoside C inhibited the growth of A549 cells, we used different inhibitors together with 0.4 μM lanatoside C. The results showed that compared with the control group, there were no statistical differences in the viability of A549 cells treated together with lanatoside C in Z-VAD-FMK group, Fer-1 group, and VX-765 group (*Figure 2A*). Compared with the control group, the LDH release significantly enhanced in lanatoside C group, namely when the control group were treated with 0.4 μM lanatoside C; Meanwhile, when A549 cells were treated with lanatoside C, the LDH release in Z-VAD-FMK group and Fer-1 group decreased significantly compared with the lanatoside C group, especially with a more reduction in Fer-1 group (*Figure 2B*). These results demonstrated that ferroptosis inhibitors were more effective in inhibiting lanatoside C-mediated cell death, so experiments focused on ferroptosis were conducted. As a result, the protein content of SLC7A11 and GPX4 by western blotting in lanatoside C group were significantly decreased compared with the control group (*Figure 2C*), and so was the fluorescence intensity by confocal microscopy (*Figure 2D,2E*). In addition, TEM and mitochondrial membrane potential detection analysis showed that the mitochondria of A549 cells in lanatoside C group disappeared (*Figure 2F*) and the mitochondrial membrane potential decreased (*Figure 2G*).

Lanatoside C suppressed the growth of lung cancer in vivo

In order to assess the anti-proliferative effect of lanatoside C *in vivo*, we established a subcutaneous tumor model in nude mice using A549 cells. The body size of the mice was not affected by tumor xenograft. However, lanatoside C efficiently inhibited the growth of xenograft tumors, as well as reducing the size and weight of the tumor (*Figure 3A-3D*). We investigated the influence of lanatoside C on cell proliferation and cell death using Ki67 immunohistochemistry and HE staining of tumor sections. We found that lanatoside C significantly suppressed the proliferation of tumor cells and enhanced tumor cell death (*Figure 3E*).

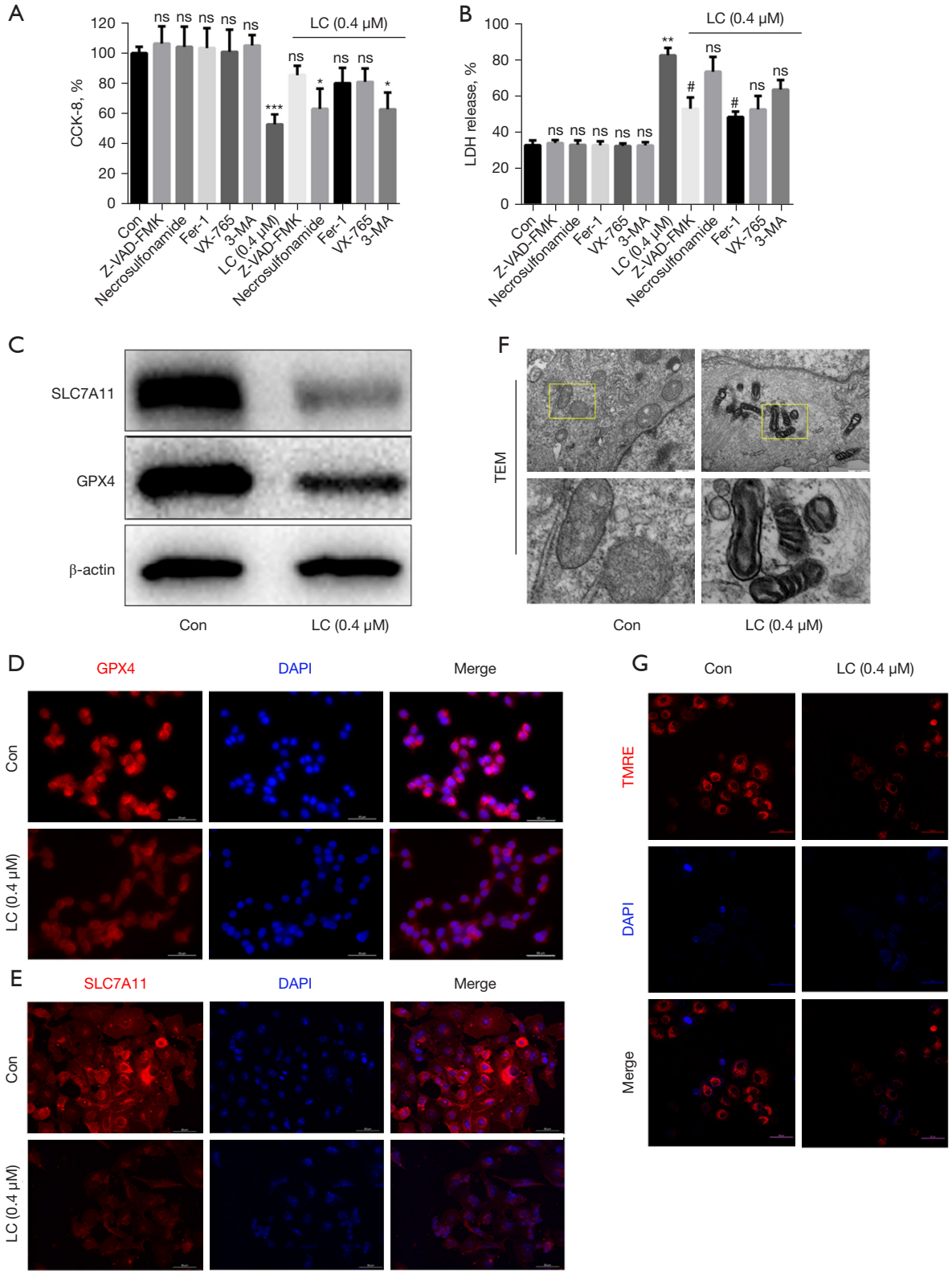

Figure 2 The effect of LC on A549 cells was induced by ferroptosis. (A) The viability of A549 cells with different inhibitors was assessed using CCK-8 assay, including Z-VAD-FMK for apoptosis, necrosulfonamide for necrocytosis, VX-765 for pyroptosis, Fer-1 for ferroptosis,

and 3-MA for autophagy, when treated with 0.4 μM LC or not. (B) The LDH release of A549 cells with different inhibitors was evaluated when treated with 0.4 μM LC or not. Compared with the con group, the LDH release significantly enhanced in LC (0.4 μM) group, and the LDH release in Z-VAD-FMK group and Fer-1 group treated with LC decreased significantly compared with LC (0.4 μM) group. (C) Protein expression of SLC7A11 and GPX4 was measured by western blotting. (D,E) Fluorescence intensity of GPX4 (D) and SLC7A11 (E) was detected by confocal microscopy. Scale bar =50 μm. (F) Analysis of mitochondria in A549 cells by TEM was performed. Scale bar =50 μm. The yellow frames in the con group showed that the inner mitochondrial structure was intact and the inner mitochondrial ridge structure was obviously visible; the yellow frames in the LC (0.4 μM) group showed the inner mitochondrial structure was destroyed, the whole mitochondrial wrinkle was shrunk, and the inner mitochondrial ridge structure disappeared, showing characteristic changes of ferroptosis. (G) Changes in mitochondrial membrane potential was assessed by TEM. Scale bar =50 μm. Data were presented as mean ± SD, and statistical significance was calculated using one-way ANOVA with Tukey's multiple comparison test. ns, P>0.05; *, P<0.05; **, P<0.01; ***, P<0.001 *vs.* Con; #, P<0.05 *vs.* LC (0.4 μM). CCK-8, cell counting kit-8; Con, control group; Fer-1, ferrostatin-1; LC, lanatoside C; LDH, lactate dehydrogenase; TEM, transmission electron microscopy; DAPI, 4,6-diamino-2-phenylindole; SD, standard deviation; ANOVA, analysis of variance.

Ferroptosis is induced by iron accumulation and lipid peroxidation, and is characterized by mitochondrial contraction. In the subcutaneous tumor model in nude mice, ferroptosis was assessed by measuring GPX4 and SLC7A11 levels. As shown in (*Figure 4A*), Immunohistochemical staining analysis revealed that the SLC7A11 and GPX4 levels significantly decreased in mice in the lanatoside C group. In addition, the expression of GPX4 and SLC7A11 protein was decreased in the lanatoside C group (*Figure 4B*). The results demonstrated mechanism by which lanatoside C suppressed tumor growth by promoting ferroptosis (*Figure 4C*).

Discussion

Lung cancer is the most common and fast-growing malignant tumor in China (20). The high ability of cancer cells to invade and metastasize is the main reason limiting the improvement of survival after lung cancer surgery (21,22). Recent studies have found that lanatoside C has potential anti-tumor cell proliferation effects, and its anti-tumor mechanism mainly focuses on induction of autophagy, cell cycle arrest and induction of cell death, and has a good inhibitory effect on liver cancer and gastric cancer (18,19,23). In this study, we evaluated the effect of lanatoside C on ferroptosis in A549 cells, the results showed that the survival of A549 cells was significantly reduced by the treatment of lanatoside C, and the dose correlation was also observed.

Ferroptosis is a newly discovered iron-dependent mode of cell death that differs from other cell death types such as autophagy, apoptosis, necrocytosis, and pyroptosis (24,25). This form of cell death is characterized by shrinking mitochondria, dense and thickened membranes, reduced activity of SLC7A11 and GPX4 proteins (26), depletion of glutathione (GSH) content, and excessive accumulation of ROS resulting in elevated lipid peroxidation on cell membranes. It has been shown that ferroptosis is also an important regulator of tumor growth (10), in which SLC7A11 and GPX4 act as central regulators. An essential mechanism of ferroptosis by GSH-dependent GPX4 reductive system in NSCLC has been concluded (27), indicating that GPX4 can convert lipid hydroperoxides to lipid alcohols combined GSH as a cofactor, and once GSH deficiency induces cysteine deficiency, GPX4 activity is directly inactivated, causing the accumulation of lipid peroxides, which in turn leads to ferroptosis (28). The system xc^-, a cystine/glutamate antiporter, is comprised of SLC7A11 and SLC3A2. SLC7A11, as a sodium-independent cystine-glutamate reverse transporter, is responsible for transporting extracellular cystine into the cell, which is then processed into cysteine, the rate-limiting substrate for GSH synthesis (29,30). A decrease in SLC7A11 may lead to a decrease in GSH, and the function of GPX4 is suppressed, contributing to the inhibition of SLC7A11/cysteine/GSH axis, ultimately triggering ferroptosis (31). In this study, we found that lanatoside C could inhibit the expression of ferroptosis-related proteins (SLC7A11 and GPX4) and promote cellular ferroptosis. It is suggested that lanatoside C can induce ferroptosis in A549 cells.

To further investigate whether the ferroptosis pathway affects the inhibitory effect of lanatoside C on A549 cells, this study first pretreated A549 cells with lanatoside C and then treated the cells with Fer-1, a specific inhibitor of ferroptosis, which is a lipophilic free radical trapping

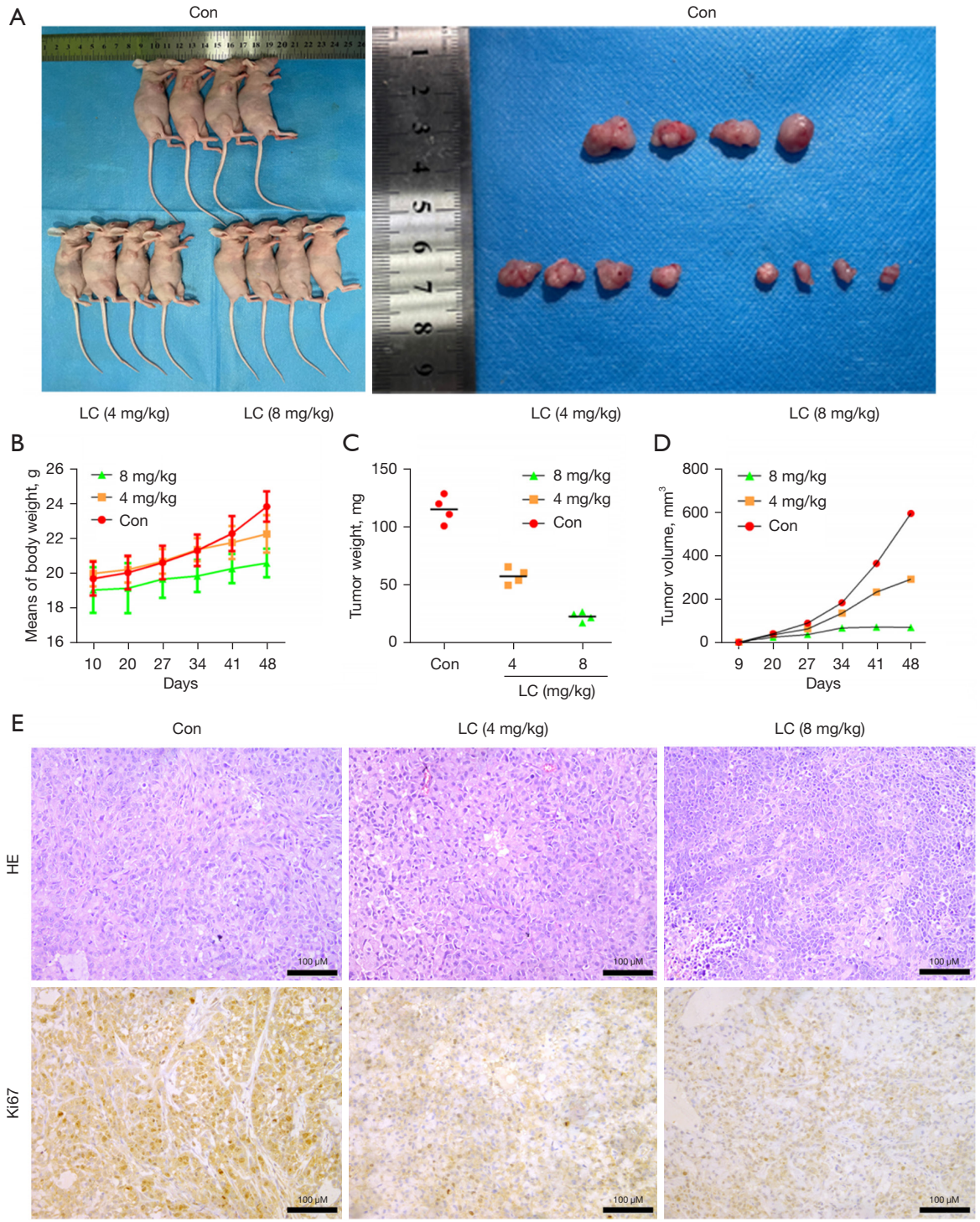

Figure 3 The analysis of the anti-proliferative effect of LC *in vivo*. (A) Body size of subcutaneous tumor model mice at different LC concentrations was calculated. (B) Means of body weight in subcutaneous tumor model mice at different LC concentrations were analyzed. (C) Tumor volume with different concentrations of LC was measured. (D) The changes of tumor volume with different concentrations of LC during the growth were figured out. (E) The results of immunohistochemistry and HE staining were monitored. Data were presented as mean ± SD, and statistical significance was calculated using one-way ANOVA with Tukey's multiple comparison test. Con, control group; LC, lanatoside C; HE, hematoxylin-eosin; SD, standard deviation; ANOVA, analysis of variance.

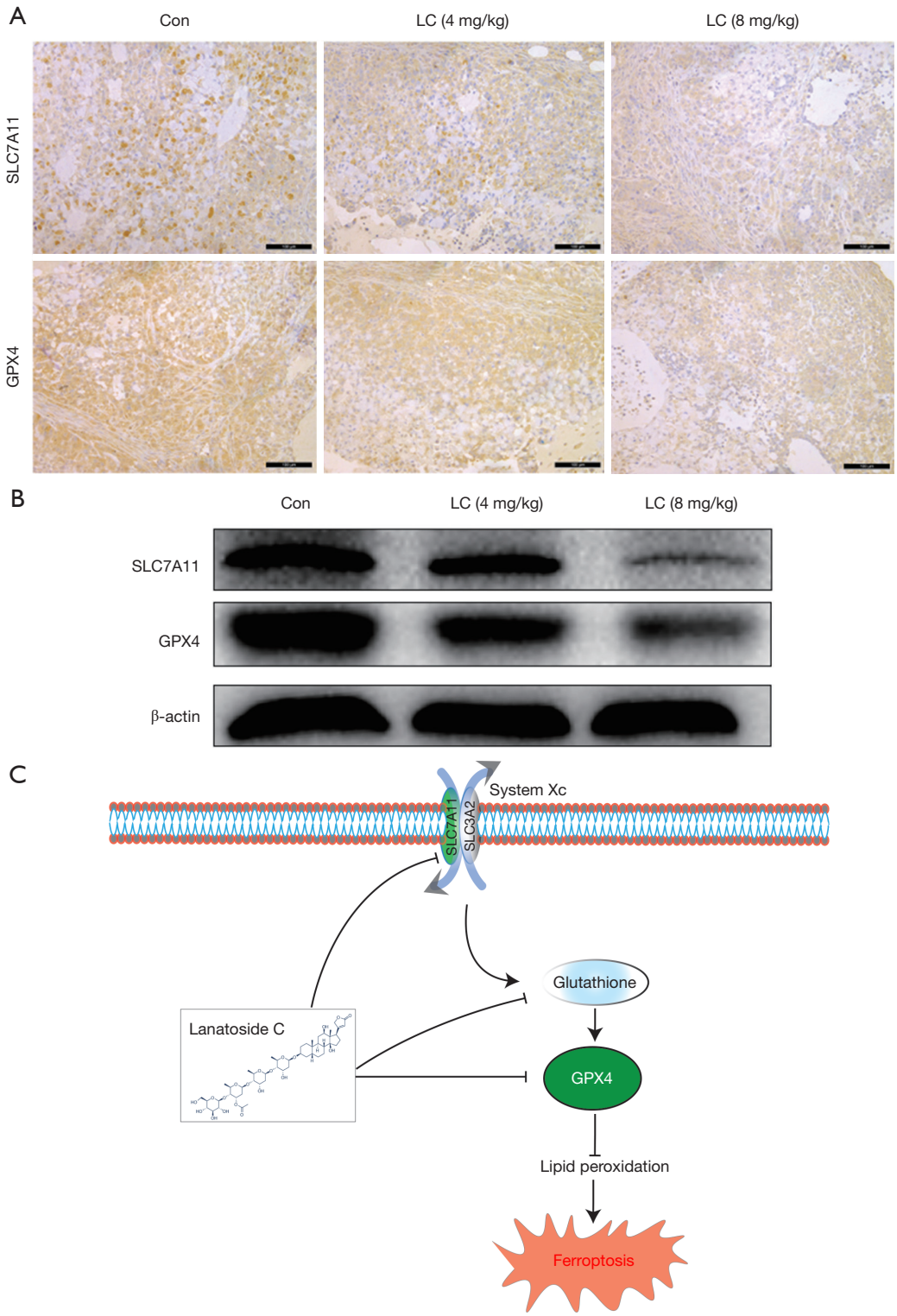

Figure 4 Ferroptosis was assessed by measuring GPX4 and SLC7A11 levels. (A) Immunohistochemical staining analysis of SLC7A11 and GPX4 was performed by Ki67 immunohistochemical staining. Scale bar =100 μm. (B) The expression of GPX4 and SLC7A11 by western blotting was detected. (C) The schematic diagram showing that LC can regulate SLC7A11/GPX4 signaling to induce ferroptosis. Con, control group; LC, lanatoside C.

antioxidant that prevents ferroptosis. The results showed that cell viability was restored in the lanatoside C + Fer-1 group compared with the lanatoside C alone group, suggesting that ferroptosis may affect the inhibition of A549 cell proliferation by lanatoside C. The effect of Fer-1, a specific inhibitor of ferroptosis, on lanatoside C-induced restoration of SLC7A11 and GPX4 protein expression in A549 cells was further investigated. The results showed that Fer-l restored the lanatoside C-induced down-regulation of SLC7 and GPX4 expression. Mitochondrial morphology and membrane potential changes are importantly linked to ferroptosis progression and can be used as markers of mitochondrial damage. In this study, Fer-l reversed lanatoside C-mediated mitochondrial damage. *In vivo* results showed that lanatoside C significantly suppressed the tumor size and weight. Ki67 is a well-known proliferation marker used to assess cell proliferation. In this study, both high and low concentrations of lanatoside C significantly decreased Ki67 expression, suggesting that lanatoside C could inhibit tumor cell proliferation, and promote apoptosis of tumor cells.

Conclusions

In summary, we found that lanatoside C exerts antiproliferative effects *in vivo* or *in vitro* by regulating SLC7A11/GPX4 signaling to induce ferroptosis. Despite these findings, one of the main limitations of this study is that the effect of lanatoside C on ferroptosis in cells has not been studied. It is concluded that lanatoside C can be considered as an anticancer agent that induces ferroptosis in the treatment of NSCLC.

Acknowledgments

We would like to thank Editage (http://www.editage.cn/) for their assistance with English language editing.
Funding: This study was funded by the National Natural Science Foundation of China (No. 81972977) and the Foundation of Health Commission of Sichuan Province (No. 20ZD016).

Footnote

Reporting Checklist: The authors have completed the ARRIVE reporting checklist. Available at https://tcr.amegroups.com/article/view/10.21037/tcr-23-2285/rc

Data Sharing Statement: Available at https://tcr.amegroups.com/article/view/10.21037/tcr-23-2285/dss

Peer Review File: Available at https://tcr.amegroups.com/article/view/10.21037/tcr-23-2285/prf

Conflicts of Interest: All authors have completed the ICMJE uniform disclosure form (available at https://tcr.amegroups.com/article/view/10.21037/tcr-23-2285/coif). The authors have no conflicts of interest to declare.

Ethical Statement: The authors are accountable for all aspects of the work in ensuring that questions related to the accuracy or integrity of any part of the work are appropriately investigated and resolved. Experiments were performed under a project license (No. CMC-IACUC-2022050) granted by the Experimental Animal Ethics Committee of Chengdu Medical College, in accordance with the Chengdu Medical College's guidelines for the care and use of animals.

References

1. Petrella F, Rizzo S, Attili I, et al. Stage III Non-Small-Cell Lung Cancer: An Overview of Treatment Options. Curr Oncol 2023;30:3160-75.
2. Öjlert ÅK, Halvorsen AR, Nebdal D, et al. The immune microenvironment in non-small cell lung cancer is predictive of prognosis after surgery. Mol Oncol 2019;13:1166-79.
3. Zhou S, Yang H. Immunotherapy resistance in non-small-cell lung cancer: From mechanism to clinical strategies. Front Immunol 2023;14:1129465.
4. Cheng F, Dou J, Yang Y, et al. Drug-induced lactate confers ferroptosis resistance via p38-SGK1-NEDD4L-dependent upregulation of GPX4 in NSCLC cells. Cell Death Discov 2023;9:165.

5. Yang WS, Stockwell BR. Ferroptosis: Death by Lipid Peroxidation. Trends Cell Biol 2016;26:165-76.
6. Ursini F, Maiorino M. Lipid peroxidation and ferroptosis: The role of GSH and GPx4. Free Radic Biol Med 2020;152:175-85.
7. Li Y, Cao Y, Xiao J, et al. Inhibitor of apoptosis-stimulating protein of p53 inhibits ferroptosis and alleviates intestinal ischemia/reperfusion-induced acute lung injury. Cell Death Differ 2020;27:2635-50.
8. Belavgeni A, Meyer C, Stumpf J, et al. Ferroptosis and Necroptosis in the Kidney. Cell Chem Biol 2020;27:448-62.
9. Wang J, Liu Y, Wang Y, et al. The Cross-Link between Ferroptosis and Kidney Diseases. Oxid Med Cell Longev 2021;2021:6654887.
10. Chen X, Kang R, Kroemer G, et al. Broadening horizons: the role of ferroptosis in cancer. Nat Rev Clin Oncol 2021;18:280-96.
11. Zhang Y, Tan H, Daniels JD, et al. Imidazole Ketone Erastin Induces Ferroptosis and Slows Tumor Growth in a Mouse Lymphoma Model. Cell Chem Biol 2019;26:623-633.e9.
12. Zhang W, Jiang B, Liu Y, et al. Bufotalin induces ferroptosis in non-small cell lung cancer cells by facilitating the ubiquitination and degradation of GPX4. Free Radic Biol Med 2022;180:75-84.
13. Gai C, Yu M, Li Z, et al. Acetaminophen sensitizing erastin-induced ferroptosis via modulation of Nrf2/heme oxygenase-1 signaling pathway in non-small-cell lung cancer. J Cell Physiol 2020;235:3329-39.
14. Ueda Y, Mishiro K, Yoshida K, et al. Regioselective diversification of a cardiac glycoside, lanatoside C, by organocatalysis. J Org Chem 2012;77:7850-7.
15. Ha DP, Tsai YL, Lee AS. Suppression of ER-stress induction of GRP78 as an anti-neoplastic mechanism of the cardiac glycoside Lanatoside C in pancreatic cancer: Lanatoside C suppresses GRP78 stress induction. Neoplasia 2021;23:1213-26.
16. Pavithran H, Kumavath R, Ghosh P. Transcriptome Profiling of Cardiac Glycoside Treatment Reveals EGR1 and Downstream Proteins of MAPK/ERK Signaling Pathway in Human Breast Cancer Cells. Int J Mol Sci 2023;24:15922.
17. Reddy D, Kumavath R, Ghosh P, et al. Lanatoside C Induces G2/M Cell Cycle Arrest and Suppresses Cancer Cell Growth by Attenuating MAPK, Wnt, JAK-STAT, and PI3K/AKT/mTOR Signaling Pathways. Biomolecules 2019;9:792.
18. Hu Y, Yu K, Wang G, et al. Lanatoside C inhibits cell proliferation and induces apoptosis through attenuating Wnt/β-catenin/c-Myc signaling pathway in human gastric cancer cell. Biochem Pharmacol 2018;150:280-92.
19. Durmaz I, Guven EB, Ersahin T, et al. Liver cancer cells are sensitive to Lanatoside C induced cell death independent of their PTEN status. Phytomedicine 2016;23:42-51.
20. Mao Y, Gao Z, Yin Y. Complete Video-Assisted Thoracoscopic Surgery and Traditional Open Surgery for Elderly Patients With NSCLC. Front Surg 2022;9:863273.
21. Iseli T, Berghmans T, Glatzer M, et al. Adverse events reporting in stage III NSCLC trials investigating surgery and radiotherapy. ERJ Open Res 2020;6:00010-2020.
22. Weder W, Furrer K, Opitz I. Robotic-assisted thoracoscopic surgery for clinically stage IIIA (c-N2) NSCLC-is it justified? Transl Lung Cancer Res 2021;10:1-4.
23. Badr CE, Wurdinger T, Nilsson J, et al. Lanatoside C sensitizes glioblastoma cells to tumor necrosis factor-related apoptosis-inducing ligand and induces an alternative cell death pathway. Neuro Oncol 2011;13:1213-24.
24. Yan HF, Zou T, Tuo QZ, et al. Ferroptosis: mechanisms and links with diseases. Signal Transduct Target Ther 2021;6:49.
25. Su LJ, Zhang JH, Gomez H, et al. Reactive Oxygen Species-Induced Lipid Peroxidation in Apoptosis, Autophagy, and Ferroptosis. Oxid Med Cell Longev 2019;2019:5080843.
26. Yuan Y, Zhai Y, Chen J, et al. Kaempferol Ameliorates Oxygen-Glucose Deprivation/Reoxygenation-Induced Neuronal Ferroptosis by Activating Nrf2/SLC7A11/GPX4 Axis. Biomolecules 2021;11:923.
27. Shui S, Zhao Z, Wang H, et al. Non-enzymatic lipid peroxidation initiated by photodynamic therapy drives a distinct ferroptosis-like cell death pathway. Redox Biol 2021;45:102056.
28. Yi R, Wang H, Deng C, et al. Dihydroartemisinin initiates ferroptosis in glioblastoma through GPX4 inhibition. Biosci Rep 2020;40:BSR20193314.
29. Sun L, Dong H, Zhang W, et al. Lipid Peroxidation, GSH Depletion, and SLC7A11 Inhibition Are Common Causes of EMT and Ferroptosis in A549 Cells, but Different in

Specific Mechanisms. DNA Cell Biol 2021;40:172-83.
30. Rosell R, Jain A, Codony-Servat J, et al. Biological insights in non-small cell lung cancer. Cancer Biol Med 2023;20:500-18.
31. Yang WS, SriRamaratnam R, Welsch ME, et al. Regulation of ferroptotic cancer cell death by GPX4. Cell 2014;156:317-31.

Cite this article as: Xia Y, Liu T, Deng S, Li L, Li J, Zhang F, He S, Yuan W, Wu D, Xu Y. Lanatoside C induces ferroptosis in non-small cell lung cancer *in vivo* and *in vitro* by regulating SLC7A11/GPX4 signaling pathway. Transl Cancer Res 2024;13(5):2295-2307. doi: 10.21037/tcr-23-2285

